

Estimating the Effect of Crosstalk Error on Circuit Fidelity Using Noisy Intermediate-Scale Quantum Computers

Sovanmonynuth Heng¹, Myeongseong Go¹, Youngsun Han^{1*}

¹Department of AI Convergence, Pukyong National University, Busan, South Korea.

*Corresponding author(s). E-mail(s): youngsun@pknu.ac.kr;

Abstract

Current advancements in technology have focused the attention of the quantum computing community toward exploring the potential of near-term devices whose computing power surpasses that of classical computers in practical applications. An unresolved central question revolves around whether the inherent noise in these devices can be overcome or whether any potential quantum advantage would be limited. There is no doubt that crosstalk is one of the main sources of noise in noisy intermediate-scale quantum (NISQ) systems, and it poses a fundamental challenge to hardware designs. Crosstalk between parallel instructions can corrupt quantum states and cause incorrect program execution. In this study, we present a necessary analysis of the crosstalk error effect on NISQ devices. Our approach is extremely straightforward and practical to estimate the crosstalk error of various multi-qubit devices. In particular, we combine the randomized benchmarking (RB) and simultaneous randomized benchmarking (SRB) protocol to estimate the crosstalk error from the correlation controlled-NOT (CNOT) gate. We demonstrate this protocol experimentally on 5-, 7-, & 16-qubit devices. Our results demonstrate the crosstalk error model of three different IBM quantum devices over the experimental week and compare the error variation against the machine, number of qubits, quantum volume, processor, and topology. We then confirm the improvement in the circuit fidelity on different benchmarks by up to 3.06x via inserting an instruction barrier, as compared with an IBM quantum noisy device which offers near-optimal crosstalk mitigation in practice. Finally, we discuss the current system limitation, its tradeoff on fidelity and depth, noise beyond the NISQ system, and mitigation opportunities to ensure that the quantum operation can perform its quantum magic undisturbed.

Keywords: crosstalk error, noisy intermediate-scale quantum (NISQ), quantum device

1 Introduction

Quantum computing may be able to solve certain intractable classical problems. Companies like IBM, Google, and Rigetti have released their quantum chips with many qubits, such as 433, 53, and 79 qubits, respectively [1–3]. However, these chips are classified as noisy intermediate-scale quantum (NISQ) hardware, which has less than one thousand qubits and suffers from inevitable noise. IBM Cloud now offers cloud-based services with 5 to 133 qubits, and services with more than a thousand qubits may appear in the next few years according to the IBM roadmap [4–6]. Moreover, quantum information processors (QIPs) have demonstrated 1 and 2-qubit quantum operations with error rates below the threshold required for fault-tolerant quantum computation (FTQC) [7–9]. A major obstacle to achieving similar low error rates in large and integrated quantum processors is the ability to maintain the crosstalk error [10, 11].

Crosstalk can increase error rates both for individual qubits and across different qubits, in which case errors are correlated [10, 12, 13]. Such correlations make error correction difficult. Optimizing the power of quantum error correction (QEC) requires an understanding of and strict control of crosstalk errors. In addition, it is one of the major sources of noise in superconducting and also trapped-ion devices [13]. It can corrupt the qubit state when multiple quantum operations are executed simultaneously. It also has a significant impact on the quantum gate error. For instance, an increase of CNOT errors up to 3 times caused by crosstalk on IBMQ Casablanca [14], while the CNOT errors increase up to 11 times caused by crosstalk on IBMQ 20 Poughkeepsie [12]. Different protocols were proposed in [15–20] to detect and characterize crosstalk in quantum devices. After we assess crosstalk, we can introduce different mitigation techniques such as modifying simultaneous CNOT operations with high crosstalk error rate to execute sequentially while trading off an increase in depth and decoherence time [19, 21–23].

Through an analysis of real quantum computer historical calibration data from different IBM devices, we observe how device crosstalk error rates correlate between different devices and how they correlate with the ordering of the qubit connectivity. We discover some correlations in which the same correlation pair in the same device offers different crosstalk error rates than the revised of those correlation pairs, which indicates that they may share the same qubit, control, or other infrastructure. Shared infrastructure by devices could be a potential failure point for users looking for reliable execution of their programs on NISQ quantum devices. For this reason, we may prefer to avoid using devices that may share all or some of the same infrastructure. We also note that many of the calibration changes do not correlate to periods when the devices might have been offline, which represents unknown reasons for the calibration changes. However, changes to the control hardware or software have an important impact on the dependability of NISQ quantum computers.

In this work, we propose a method to efficiently estimate the crosstalk error from the correlation controlled-NOT (CNOT) gate by combining Randomized Benchmarking (RB) and Simultaneous Randomized Benchmarking (SRB) [24] on different quantum device properties. We initiate by preprocessing the controlled-not (CNOT) error pairing essential for characterizing crosstalk errors based on device properties.

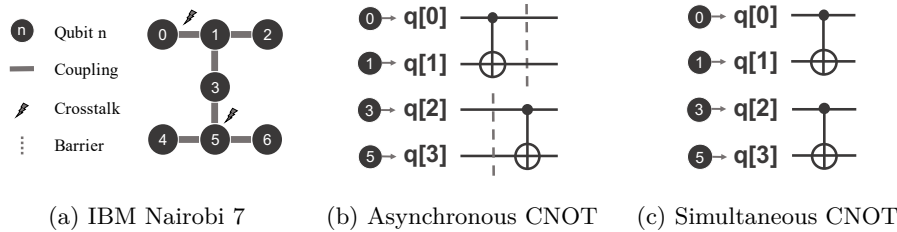


Fig. 1: Example of the crosstalk error effects characterization using IBM Nairobi 7-qubits connectivity on crosstalk correlation pair between logical-to-physical qubit mapping of $\{q[0] \rightarrow Q0, q[1] \rightarrow Q1\}$ & $\{q[2] \rightarrow Q3, q[3] \rightarrow Q5\}$.

We then present crosstalk error model variation on each device during an experimental week. Second, we evaluate the crosstalk error model on different devices in terms of machine, number of qubits, quantum volume, processor, and topology. Finally, we insert crosstalk error pairs on devices to show their impact on output circuit fidelity. We also demonstrate the fidelity improvement on various quantum circuit benchmarks and compare it with the results when an instruction barrier is inserted between the simultaneous crosstalk error pair. To this end, the following contributions are made in this paper.

- We validate the presence of crosstalk on three different IBM quantum devices by combining randomized benchmarking (RB) and simultaneous randomized benchmarking (SRB) protocols on several experimental simulations.
- We model and evaluate the dynamic of the crosstalk error models by comparing the error variations against the machine, number of qubits, quantum volume, processor, and topology of the IBM quantum devices.
- We demonstrate its impact on the output fidelity and the improvement of the circuit fidelity on various quantum benchmarks with up to 3.06x with the insertion of an instruction barrier.

This paper is organized as follows. Section 2 briefly discusses the background noise in the NISQ computers, especially crosstalk errors. Section 3 introduces related works on crosstalk error characterization using different techniques that motivate our study. Section 4 explains our methodology for addressing crosstalk on different devices. Section 5 presents a detailed evaluation of the crosstalk error rate results. Section 6 discusses the limitations and issues beyond current NISQ devices. We conclude our study in Section 7.

2 Background

This section explains the primer concept of quantum bits (qubits) and quantum gates, various kinds of noise in NISQ computers, quantum device topologies, and the crosstalk error in NISQ devices.

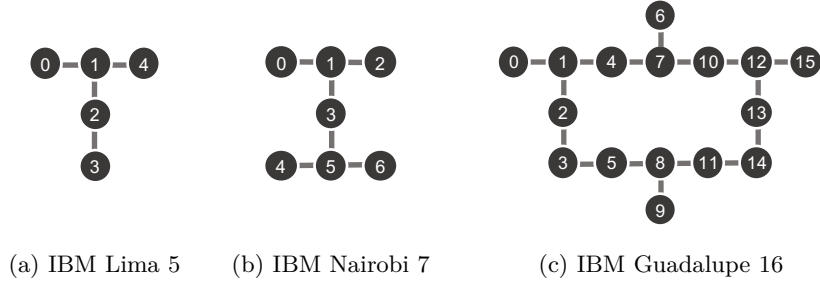


Fig. 2: IBM quantum devices with its connectivity.

2.1 Primer on Qubits and Quantum Gates

Quantum bits, or qubits $|\psi\rangle$, represent the fundamental units of quantum information in quantum computing paradigms. In stark contrast to classical bits, qubits exhibit the phenomenon of superposition, which enables them to concurrently exist in states of $|0\rangle$, or $|1\rangle$, and/or both, until they are subjected to a measurement operation [25–27]. Quantum gates, which are pivotal components in quantum computing frameworks, diverge significantly from their classical counterparts. While classical logic gates operate deterministically based on input states, quantum gates leverage the unique attributes of quantum mechanics. Quantum gates employ the principles of superposition and entanglement to execute operations on qubits, thereby enabling transformations that transcend classical logical constraints [28, 29]. Prominent among quantum gates are the Hadamard gate, which is a catalyst for the generation of superposition $|\psi\rangle = \alpha|0\rangle + \beta|1\rangle$, and the CNOT gate, which facilitates qubit entanglement $|\psi\rangle = |\psi_1\rangle \otimes |\psi_2\rangle$ as shown in Figure 1b and 1c. These gates serve as quantum analogs to the classical logic gates, and they manipulate the quantum states of qubits to affect computational processes.

2.2 Noise in the NISQ Computer

The intricacies of noise in NISQ computers unfold across various dimensions, each contributing to the formidable challenges inherent in quantum computation. The coherence error [30] reflects the susceptibility of the qubit to environmental factors and captures the gradual loss of quantum coherence over time. Measurement errors [31] stem from detector imperfections and signal noise to compound the challenges of obtaining precise quantum outcomes. Concurrently, two-qubit gate errors [31] arise from imperfections in the execution of quantum gates which introduce inaccuracies in state transformations. Single-qubit gate errors [31] result from imperfections in the implementation of operations on individual qubits. While decoherence noise poses a formidable threat, resulting from interactions between qubits and their external environment. Among the above types, a significant source of noise is two-qubit gates that face challenges stemming from imperfect entanglement operations namely crosstalk noise or error [10, 12, 13]. It exacerbates errors through unwanted interactions between neighboring qubits during quantum operations.

2.3 Quantum Device Topology

The quantum device topologies of IBM’s Lima 5 [32, 33], Nairobi 7 [34], and IBM Guadalupe 16 [35–37] in Figure 2 represent noteworthy advancements in quantum computing architecture, specifically delineating dissimilar connectivity patterns within these quantum processors. These three topologies are popular in research to address many emerging problems in practical application. Figure 2a shows IBM Lima 5 exhibiting a topological configuration characterized by five qubits and their corresponding interconnections, which reflects the intricacies of quantum entanglement and gate operations. Similarly, Figure 2b shows the IBM Nairobi 7-qubit topology, which manifests an expanded quantum processor with an intricate connectivity matrix. The connectivity within these devices is established through two-qubit gates, enabling entanglement operations between adjacent qubit pairs. On top of that, Figure 2c shows the IBM Guadalupe 16-qubit topology based on the latest heavy-hex lattice, which can provide a better quantum volume. The topologies are guided by the principles of QEC and qubit coupling and help orchestrate quantum computations within the constraints of physical qubit relations. By elucidating these patterns of connectivity, these types of quantum device topologies contribute significantly to our understanding and optimization of quantum algorithms and error mitigation strategies [38–40].

2.4 Crosstalk Error in the NISQ

Crosstalk error in quantum computing refers to unwanted interaction or interference between qubits, during quantum operations [10, 12, 13]. It arises from the imperfect isolation of quantum components, and it leads to unintended effects on neighboring qubits, thereby compromising the fidelity of quantum computations. Characterizing crosstalk errors is paramount to the comprehensive assessment and improvement of quantum processors.

One prevalent technique for quantifying crosstalk errors is quantum state tomography (QST) [18] which involves the reconstruction of the full quantum state through a series of measurements. This technique allows for a detailed examination of the density matrix, revealing crosstalk-induced deviations from the ideal quantum states. Positive operator-valued measure (POVM) techniques [18] also contribute to crosstalk error analysis by characterizing the measurement processes. POVM enables a more nuanced understanding of measurement-induced errors and crosstalk effects, enhancing the overall comprehension of the quantum information processing landscape. Among others, the randomized benchmarking (RB) protocol [16] is the most straightforward technique as an estimated protocol in QIP. The RB protocol evaluates the average fidelity of quantum gates by subjecting them to random sequences of Clifford group gates and provides a robust measure of the global error rate. The simultaneous randomized benchmarking (SRB) protocol [17] extends this methodology to concurrently assess multiple gates of $\mathcal{E}(g_i)$ or $\mathcal{E}(g_j)$, offering insights into the collective impact of crosstalk errors on the diverse gate operations of $\mathcal{E}(g_i | g_j)$. If the crosstalk error exists between them, the relation between independent and correlated errors should comply with $\mathcal{E}(g_i | g_j) > \mathcal{E}(g_i)$ or $\mathcal{E}(g_j | g_i) > \mathcal{E}(g_j)$.

To calculate the rate of the correlated error to independent error as an indicator of the crosstalk effect on CNOT pairs, we used the following Equation 1.

$$r(g_i | g_j) = \mathcal{E}(g_i | g_j) / \mathcal{E}(g_i) \quad (1)$$

These RB and SRB protocols can be used in as many iterations as possible to estimate the most scalable and accurate CNOT error rate because CNOT errors vary with each calibration on different devices [41–43].

3 Related Work and Motivation

Crosstalk error in quantum systems has been studied extensively in recent years with its opportunity in terms of mitigation techniques [15–17, 44, 45].

Some studies like [18] employed the quantum mechanics’ physiology of the positive operator-valued measure (POVM) to quantify crosstalk error and define the nature of the error. Similarly, [10] measured and characterized crosstalk by focusing on its impact on the simultaneous gate operations. This study focuses on the theoretical analysis of crosstalk error of a low-priority qubit type of error which is the single qubit (like X) and two-qubit (like CZ).

Moreover, the techniques used in studies [11, 15, 17, 46, 47] to detect or characterize crosstalk error involve quantum tomography methods such as gate set tomography, idle tomography, process tensor tomography, and parallel tomography. Even though this technique produces high accuracy on the crosstalk error rate, it requires significant computational complexity to measure crosstalk errors, and it is hard to scale up when the number of qubits grows.

Furthermore, some studies have characterized and analyzed crosstalk error properties by applying the benefit of the Randomized Benchmarking (RB) and Simultaneous Randomized Benchmarking (SRB) protocol [16, 20, 45]. Despite this study using RB and SRB protocol which is low complexity and resource efficiency to estimate the crosstalk error, each study used only one device for their experiment. Niu et al. [16] employs RB to evaluate the performance of individual quantum gates, followed by SRB to assess correlated error rates. This method offers a valuable degree of crosstalk occurring between specific pairs of gates, but it was verified on only quantum devices with 7 qubits. Similarly, Ash et al. [20] and Guan et al. [45] focus exclusively on systems with a small number of qubits which is 5 qubits devices of IBM Essex and IBM Manila, respectively.

Most of the aforementioned studies [15–20, 44, 45] were conducted ultimately to apply their proposed mitigation technique. As a result, these methods may not necessarily address the intricate dynamics of crosstalk errors and their impact on different devices. In addition, [15–20] are out-of-date data since crosstalk error is a very emerging type of error that requires up-to-date data to address its effect from various machines’ properties.

The motivation behind this study stems from the most challenging first task of realizing how much error rate on each pair and how much error rate we will face if we do not mitigate it. Crosstalk errors pose a significant obstacle to the reliable operation of quantum systems and we believe that not all crosstalk error rates on different devices

of multiple qubits are created equal. By deepening our understanding of crosstalk error properties and balancing between accuracy, method complexity, resource efficiency, and scalability of the protocol, we aim to estimate the presence of the crosstalk error effect to see the dynamic on various IBM quantum devices in this study.

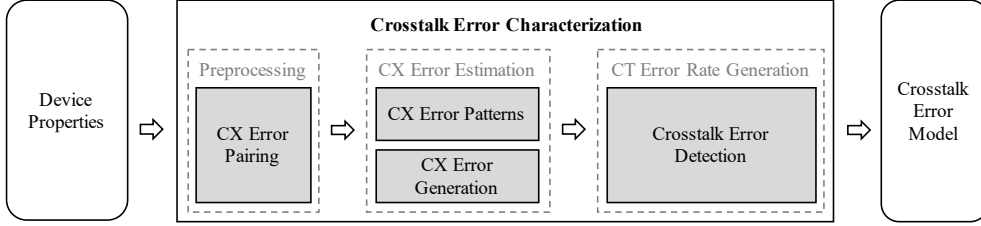


Fig. 3: Overall protocol of crosstalk error characterization to construct the crosstalk error model based on different device properties.

4 Proposed Methodology

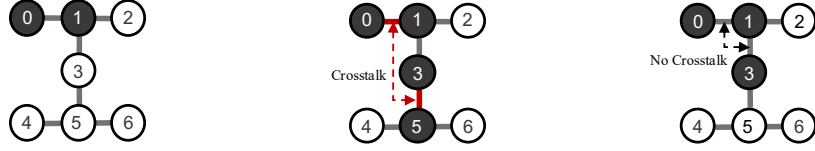
In this section, we will discuss the overall protocol we used to estimate the effect of the crosstalk error for different devices and the detailed technique used for crosstalk characterization.

4.1 Overall Protocol

Figure 3 illustrates the overall protocol of crosstalk error characterization used to construct a crosstalk error model. We divide the scheme into three distinct components namely device properties, crosstalk error characterization, and crosstalk error model. We begin with the desired device properties as the input to characterize the crosstalk error model. The choice of selecting the device will produce different crosstalk error models. For example, if you select the device as a 7-qubit machine, the crosstalk error model will produce the correlation pairs corresponding to the 7-qubit pairs. The main center rectangle part of the crosstalk error characterization is further divided into three sub-sections namely preprocessing, CNOT (CX) error estimation, and crosstalk (CT) error rate generation. The left sub-section is the preprocessing part which is required to find all possible crosstalk pairs based on the selected device properties which we name crosstalk error pairing (more detail in Section 4.2). Following preprocessing, the patterns are paired in a systematic manner suitable for identifying individual CNOT errors and simultaneous CNOT errors using Randomized Benchmarking (RB) and Simultaneous Randomized Benchmarking (SRB), respectively. Then, we can estimate each CNOT error type (more detail in Section 4.3). After that, we used the result from this step to detect whether there is a crosstalk error occurred and generate its severity on each correlation pair of the crosstalk (more detail in Section 4.4). Then we can accumulate the effect of the crosstalk error and construct the model on the device’s unique characteristics.

4.2 Preprocessing

Based on the selected device, we can preprocess all possible crosstalk error pairs as input to estimate the CNOT error. Khadirsharbiyani et al. [48] stated that if two qubits do not have simultaneously running CNOTs, no crosstalk occurs. Hence, we use these rules of no duplicate qubits in our experiment to estimate the crosstalk error effect. For instance, Figure 4 shows how we set up the preprocessing step on qubit pair on IBM Nairobi with a 7-qubit topology. We begin by selecting the qubit pair of interest like $Q[0, 1]$ in Figure 4a. Then, we pair a crosstalk scenario between the qubit of interest $Q[0, 1]$ and another qubit $Q[3, 5]$ as Figure 4b. The qubits are implicated as crosstalk and connected by a red dashed line, with the word "Crosstalk" explicitly marked to denote the interaction between them. Besides this example pair, the crosstalk can occur between $Q[0, 1]$ & $Q[4, 5]$ and $Q[0, 1]$ & $Q[5, 6]$ as well. Figure 4c illustrates a scenario where there is no crosstalk. It demonstrates the relationship between the qubit of interest $Q[0, 1]$ and a neighboring qubit $Q[1, 2]$ & $Q[1, 3]$, connected by a black dashed line to indicate their association. In contrast to the crosstalk scenario, this connection is labeled "No Crosstalk," indicating that there is no crosstalk error present between these kinds of two qubits correlation pairs. Since we cannot execute this pair simultaneously to address the crosstalk error. By following this rule for all qubits of interest on this device, we identify and differentiate between paired qubits with crosstalk and those without on IBM Nairobi.



(a) Qubit pair of interest (b) Pair of $Q[0, 1]$ & $Q[3, 5]$ (c) Unpair of $Q[0, 1]$ & $Q[1, 2]$

Fig. 4: Preprocessing to address the crosstalk pair based on the example machine IBM Nairobi 7 qubits device on (a) qubit of interest $Q[0, 1]$ with (b) pair of crosstalk between $Q[0, 1]$ & $Q[3, 5]$, while (c) is an unpair of crosstalk between $Q[0, 1]$ & $Q[1, 2]$.

4.3 Crosstalk Error Estimation

To estimate the effect of the CNOT error pair from the preprocessing step, we create a circuit with the CNOT error pattern of both individual and simultaneous CNOT pairs randomly generated by the RB and SRB protocols, respectively. Algorithm 1 describes the operation of estimating the CNOT error using the RB and SRB protocol. The algorithm begins by deciding the necessary input components such as the number of qubits (nQ) with the basic gates (bG) of the target device, the number of seeds (nS) with the number of Clifford group gates (nC) needed for the RB and SRB protocol, and CNOT correlation pair 1 ($P1$), and pair 2 ($P2$) from the preprocessing step. The

Algorithm 1 CNOT Error Estimation

Input:

nQ : number of qubits used,
 bG : the basic gate of the target device,
 nS : number of seeds used,
 nC : number of Clifford group gates,
 $P1$: a list of CNOT pair 1,
 $P2$: a list of CNOT pair 2,

Output:

epg : a list of errors per gate on individual and simultaneous CNOT

```
1: procedure ESTIMATE_CNOT_ERROR( $nQ, bG, nS, nC, P1, P2$ )
2:    $pattern \leftarrow$  empty list;
3:    $epg \leftarrow$  empty list
4:   for  $pair1 \in P1$  do                                      $\triangleright$  Loop through pairs in  $P1$ 
5:     for  $pair2 \in P2$  do                                      $\triangleright$  Loop through pairs in  $P2$ 
6:       for  $i \in \{0, 1, 2\}$  do
7:         if  $i = 0$  then
8:            $nQ \leftarrow 2$ 
9:            $pattern = [pair1]$ 
10:        else if  $i = 1$  then
11:           $nQ \leftarrow 2$ 
12:           $pattern = [pair2]$ 
13:        else
14:           $nQ \leftarrow 4$ 
15:           $pattern = [[pair1], [pair2]]$ 
16:        end if
17:      end for
18:      for  $P \in pattern$  do                                      $\triangleright$  Loop through elements in  $pattern$ 
19:         $circuit \leftarrow$  ApplyRBSequence( $nS, nC, bG, P$ )
20:         $epc \leftarrow$  GetErrorPerClifford( $circuit$ )
21:         $epg \leftarrow epc/1.5$ 
22:      end for
23:    end for
24:  end for
25:  return  $epg$ 
26: end procedure
```

output of the algorithm will be a list of errors per gate on individual and simultaneous CNOT as (epg). We begin the procedure name “ESTIMATE_CNOT_ERROR” with inputs of $nQ, bG, nS, nC, P1, P2$. Then, we initialize an empty list of $pattern$ to store the current pattern being generated and an empty list of epg to store the error per gate output result. It iterates through each pair $pair1$ in $pair2$ of CNOT pair lists from $P1$ and $P2$. For each pair, we iterate three times to alter the number of qubits used in the pattern accordingly. In the first two iterations, the simulation used only two qubits of RB protocol to address two different individual CNOT error patterns of

[*pair1*] and [*pair2*]. The last iteration used four qubits of SRB protocol to address two simultaneous CNOT error patterns of [[*pair1*], [*pair2*]]. After generating the pattern, we can generate the CNOT error. For each pattern, we create a circuit by applying the RB sequence with the given number of seed (nS), number of Clifford group gate (nC), basic gate (bG), and its current pattern. Based on this circuit, we can compute the error per Clifford (epc) using the *GetErrorPerClifford*. We scaled the error per gate of CNOT by 1.5 following the previous studies [49, 50]. Then this algorithm returns each generated epg in the pattern.

4.4 Crosstalk Error Rate Generation

As we mentioned in Section 2.4, we delve into the phenomenon of crosstalk, which arises when gates are executed simultaneously on specific pairs of hardware topology within quantum computing systems. In this paper, we defined the crosstalk effect as a crosstalk error rate (r_{SRB}). This metric is fundamental to our analysis and is calculated as the ratio of the simultaneous CNOT gate error (\mathcal{E}_{SRB}) to the individual CNOT gate error (\mathcal{E}_{RB}) obtained through our extensive experimentation. Formally, this association is expressed as:

$$r_{SRB} = \mathcal{E}_{SRB} / \mathcal{E}_{RB} \quad (2)$$

To determine the presence of crosstalk, we conduct a comparison between the error incurred when executing simultaneous CNOT gates (\mathcal{E}_{SRB}) and the errors observed during individual CNOT gate operations (\mathcal{E}_{RB1} and \mathcal{E}_{RB2}). If the error during simultaneous CNOT operations is higher than either of the errors during individual CNOT gate operations, it suggests there is a crosstalk within that specific pair of hardware connections. Conversely, if the error during simultaneous CNOT operations does not surpass that of individual CNOT gate operations, it implies coherence between the error profiles of simultaneous and individual executions. In such instances, we conclude that crosstalk has not manifested within that particular correlation pair.

5 Evaluation

In this section, we discuss our experimental setup and evaluate the RB and SRB protocols by presenting our crosstalk error model, daily variation in the crosstalk error, comparing the dynamic of the crosstalk error model, and illustrating the impact of crosstalk error on several benchmark circuits using three IBM quantum devices.

5.1 Experimental Setup

To facilitate our evaluation, we present an experimental setup for addressing the crosstalk error simulation.

Backend: We select three different IBM quantum devices namely IBM Fake LimaV2 with 5 qubits, IBM Fake NairobiV2 with 7 qubits, and IBM Fake GuadalupeV2 with 16 qubits as the backend for the experiment depending on the type of machine, number of qubits, quantum volume, processor, and topology of each device.

Experimental Circuit: We use random circuits for randomized benchmarking (RB) with a default of 1024 shots and n number of qubits based on the device’s basic gates. In each experimental circuit layer, we randomly combined 150 Clifford group gates in the circuit layer together and ran them for 5 iterations (5 seeds). Each iteration includes 8 subcircuits, so we have 40 subcircuits to execute and calculate the average number of Errors Per Gate (EPG). Many qubit errors, particularly crosstalk errors, are not apparent in low-width circuit layers; thus, studying low-width circuit layers is insufficient. Hence, our goal is to scale the RB and SRB to quantify the average error in high-width circuit layer sets.

Baselines: An asynchronous circuit of CNOT is used as the baseline for comparison with the number of CNOT insertions simultaneously into the circuit.

Benchmark: We select a small-scale circuit as a benchmark that fits in with our IBM quantum devices to validate the fidelity, namely `grover_n2`, `toffoli_n3`, `cat_state_n4`, and `Ipn_n5`.

5.2 Crosstalk Error Models

To illustrate the presence of crosstalk error, we conducted an experiment using three distinguishing IBM quantum devices. For a fair result, Figure 5 presents the average crosstalk error characterization on each IBM quantum device over 5 consecutive days. A correlation pair with no color is a correlation pair with no crosstalk because it contains duplicate qubits, such as $Q[0, 1]$ & $Q[0, 1]$ or $Q[1, 2]$ & $Q[0, 1]$, whereas the color black indicates a correlation pair with crosstalk error based on its variation mode.

Figure 5a shows the average crosstalk error rate for IBM Lima 5. From these results, we can see that the crosstalk correlation pair with the minor error pair is $Q[3, 4]$ & $Q[1, 2]$ because it is whiter in color and the most severe is $Q[1, 2]$ & $Q[3, 4]$ because it is darker in color. In addition, Figure 5b shows the average crosstalk error rate for IBM Nairobi 7. It shows more crosstalk correlation pairs because it uses 7 qubits in this topology. The minor error pairs are $Q[3, 5]$ & $Q[1, 2]$, and $Q[4, 5]$ & $Q[1, 2]$, whereas the most severe is the pair $Q[1, 2]$ & $Q[3, 5]$. Since IBM Guadalupe has 16 qubits, Figure 5c shows the average crosstalk error rate in many correlation pairs. The minor error pairs are $Q[2, 3]$ & $Q[7, 10]$, and $Q[10, 12]$ & $Q[1, 4]$. In contrast, the most severe pair is between $Q[1, 4]$ & $Q[10, 12]$.

This result shows the crosstalk correlation pair varies depending on the pair selected for the operation. Even the same pair with the reverse of the qubit pair can also create a very different crosstalk error rate. Notably, the ascending number of qubit orders usually got a higher crosstalk effect on the operation. For example, $Q[1, 2]$ & $Q[3, 4]$ are more severe than $Q[3, 4]$ & $Q[1, 2]$ on IBM Lima 5, $Q[1, 2]$ & $Q[3, 5]$ are more severe than $Q[3, 5]$ & $Q[1, 2]$ on IBM Nairobi 7, and $Q[1, 4]$ & $Q[10, 12]$ are more severe than $Q[10, 12]$ & $Q[1, 4]$ on IBM Guadalupe 16. Hence, all devices’ average crosstalk error rates show that the upper-right correlation pair is darker in black, which indicates the severity of the crosstalk error pair. In contrast, the bottom left is lighter in color, which indicates a minor crosstalk error pair.

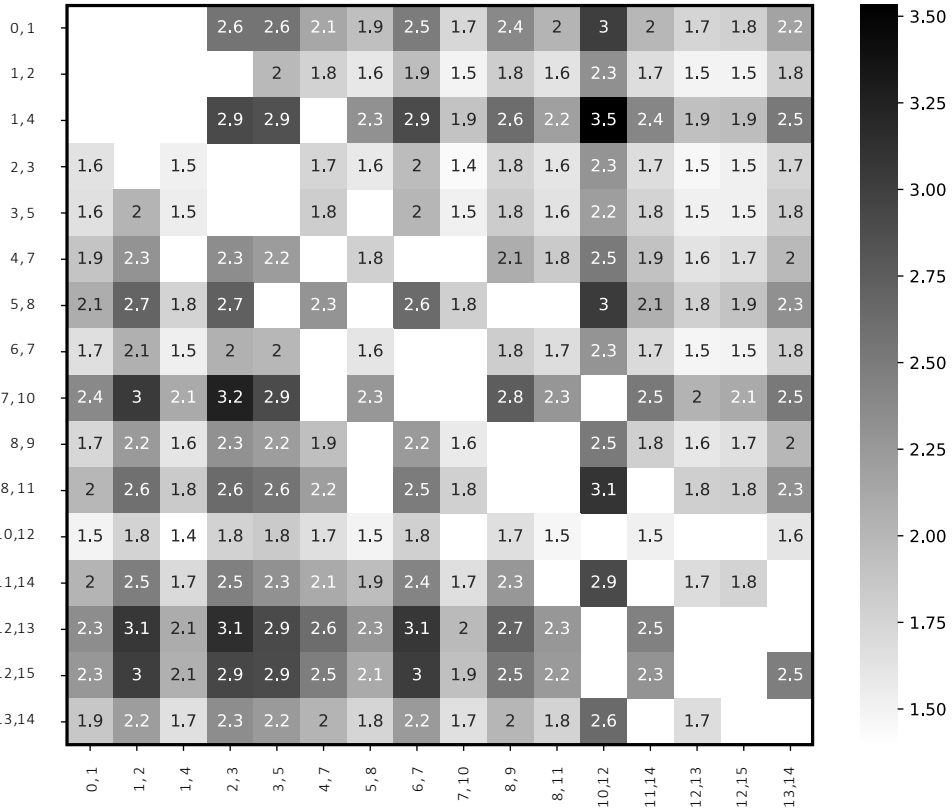
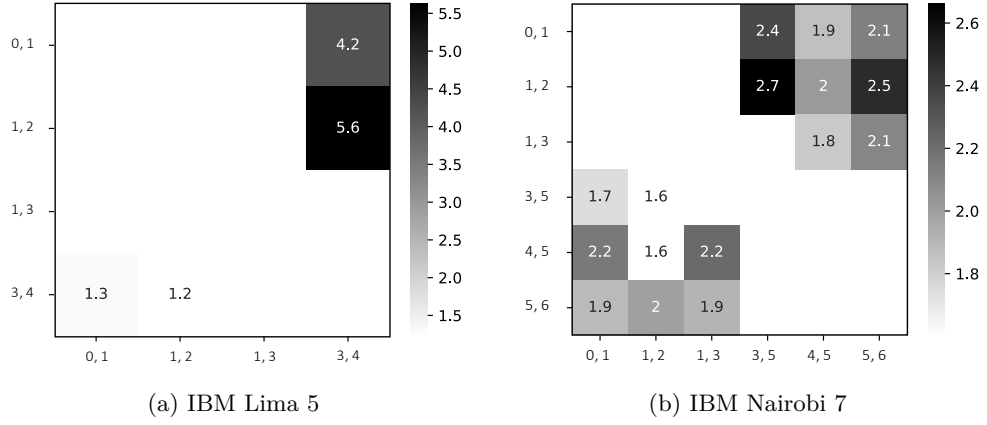
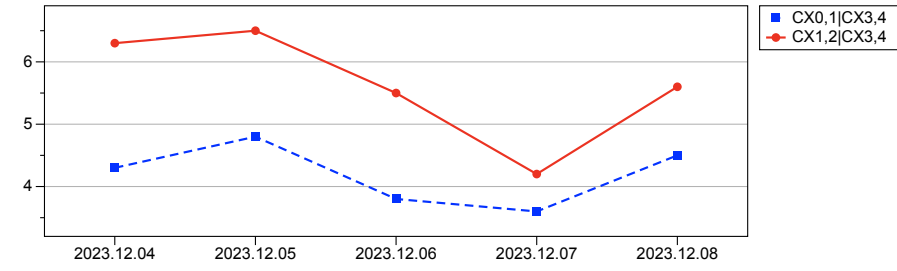
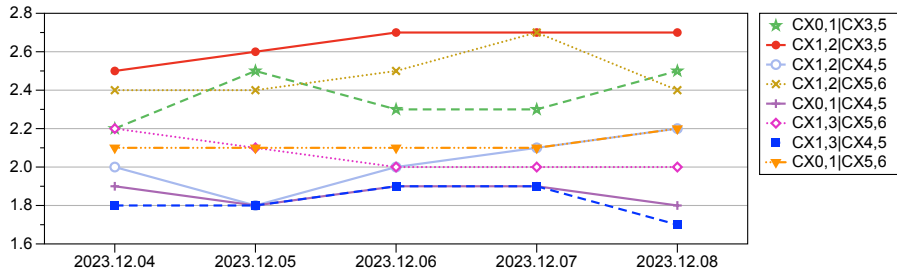


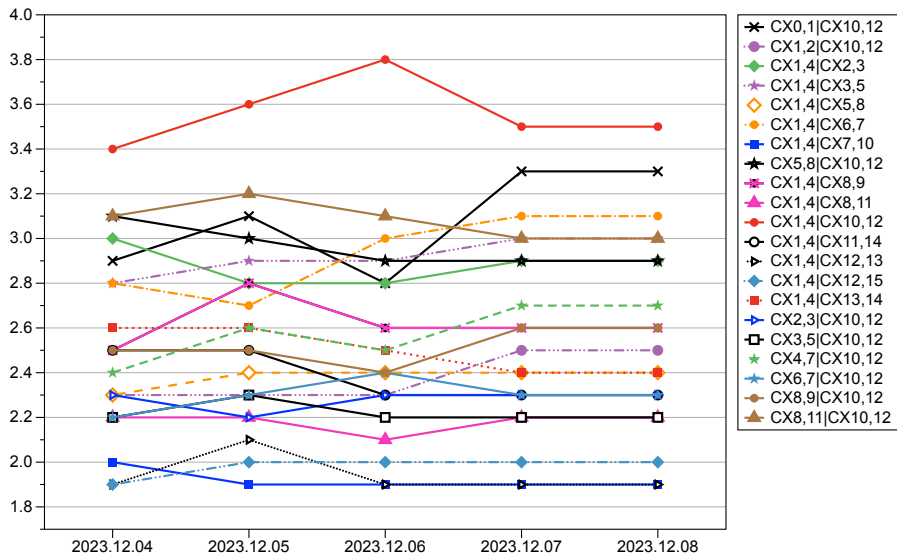
Fig. 5: Average crosstalk error model for different IBM quantum devices. The x-axis and y-axis represent the pairwise correlation between qubit pairs 1 and 2, respectively. A black color indicates a higher crosstalk error rate on all devices.



(a) IBM Lima 5



(b) IBM Nairobi 7



(c) IBM Guadalupe 16

Fig. 6: Daily variation in crosstalk error rate for three different IBM quantum devices. The x-axis represents the five consecutive days of experimentation, and the y-axis represents the crosstalk error rate. Each line with a marker represents a distinguished individual crosstalk correlation pair on the devices.

5.3 Daily Variation in Crosstalk Error

To illustrate the daily variation in the crosstalk error, we present the daily variation in the crosstalk error rate for 5 consecutive days starting from December 4, 2023 to December 8, 2023 using three different IBM quantum devices. Figure 6 shows the daily variation in the crosstalk error rate on IBM Lima 5, IBM Nairobi 7, and IBM Guadalupe 16. This variation indicates the consistency for the same device even though we performed experiments on different days. The consistency refers to the level of the crosstalk correlation pairs behaved among other pairs. The line on all pairs (all devices) seems to go up and down; this variation corresponds to the updated calibration data provided by the IBM cloud services.

Figure 6a shows the daily variation in the crosstalk error rate for IBM Lima 5. The severe crosstalk correlation pair of $Q[1, 2]$ & $Q[3, 4]$ is colored in the red solid line with the circle markers. The minor crosstalk correlation pair of $Q[0, 1]$ & $Q[3, 4]$ is colored in the blue dotted line with the square markers. The daily variation in the crosstalk error rate varies up to 4.66x on average (1.2 to 5.6) for IBM Lima. Figure 6b shows the daily variation in the crosstalk error rate for IBM Nairobi 7. The severe crosstalk correlation pair of $Q[1, 2]$ & $Q[3, 5]$ is a red solid line with circle markers. The minor crosstalk correlation pair of $Q[1, 3]$ & $Q[4, 5]$ is colored in the blue dotted line with square markers. Among others, we observe that the crosstalk correlation pairs of $Q[0, 1]$ & $Q[5, 6]$, which are shown as the orange solid line with the triangle markers are the most consistent from December 4, 2023 to December 7, 2023. The daily variation in the crosstalk error rate varies up to 1.68x on average (1.6 to 2.7) for IBM Nairobi. Figure 6c shows the daily variation in the crosstalk error rate for IBM Guadalupe 16. The severe crosstalk correlation pair of $Q[1, 4]$ & $Q[10, 12]$ is a red solid line with circle markers. The minor crosstalk correlation pair of $Q[1, 4]$ & $Q[7, 10]$ is colored in the blue dotted line with square markers.

This daily variation indicates that not all crosstalk correlation pairs behave quite the same way on every single day of the experiment. However, it does indicate that the severe pairs are still severe and the minor pairs are still minor pairs. We note that the variation for IBM Nairobi 7 is extremely low compared with the IBM Lima 5. This lower crosstalk error on IBM Nairobi 7 over the IBM Lima 5 indicates the alignment with the quantum volume (QV) in which the QV is the metric that measures the capabilities and error rates of quantum devices. Hence, the IBM Nairobi 7 has a greater QV than the IBM Lima 5. While IBM Guadalupe 16 tends to be the compromise device among the three IBM quantum devices on the crosstalk error rate.

5.4 Crosstalk Error Model Comparison

Table 1 summarizes the effect of crosstalk error for different configurations of 5-, 7-, and 16-qubit devices by three different studies by Niu et al. [16], Guan et al. [45], and our proposed method.

Niu et al. [16] offers a valuable degree of crosstalk occurring between specific pairs of gates, but it was verified on only quantum devices with 7 qubits. This study documents an escalation in the impact levels of crosstalk categorizing them as minor,

	5 Qubits	7 Qubits	16 Qubits
[16] Niu et al.	-	✓	-
Minor	-	1.5%	-
Medium	-	2.25%	-
Severe	-	3.0%	-
[45] Guan et al.	✓	-	-
Minor	1.3%	-	-
Medium	3.05%	-	-
Severe	4.8%	-	-
Our proposed	✓	✓	✓
Minor	1.2%	1.6%	1.4%
Medium	3.4%	2.15%	2.25%
Severe	5.6%	2.7%	3.1%

Table 1: Comparison of crosstalk error rates for different configurations of 5-, 7-, and 16-qubit devices.

medium, and severe, with corresponding error rates of 1.5%, 2.25%, and 3.0%, respectively. Similarly, Guan et al. [45] focuses exclusively on systems with a small number of qubits which is 5 qubits devices of IBM Manila, indicating error rates of 1.3%, 3.05%, and 4.8% corresponding to minor, medium, and severe impact levels, respectively. This suggests that their method may not be sufficiently comprehensive for addressing crosstalk across various quantum computing platforms.

Differently from the existing methods, our proposed method presents a robust protocol functioning across three different numbers of qubit devices, showing not only versatility but also competitive percentages in error rates or efficiency levels. The percentages vary for different levels of impact (minor, medium, severe) and increase with the complexity of the quantum system indicated by the number of qubits. Our study illustrates the comprehensive applicability and effectiveness of the protocol in different scenarios, highlighting how each fares in terms of scalability and efficiency across different sizes of dynamic quantum systems.

Table 2 shows the detailed crosstalk error model for three different IBM quantum devices in terms of machine, number of qubits (#Qs), quantum volume (QV), processor, crosstalk mode (CT Mode), and topology. Within the IBM Lima architecture, a Falcon r4T configuration contains five qubits carefully arranged in a T topology connectivity. Contrary to expectations, the crosstalk error model exhibited by these arrangements surpasses that observed for the IBM Nairobi device. It is noteworthy that despite the modest number of qubits (just five) and a QV of eight, the Falcon r4T configuration on IBM Lima experiences a significantly more pronounced crosstalk error. The severity of the crosstalk error on this machine is approximately 2.5x greater than that encountered on the IBM Nairobi. Although the new Falcon r5.1H IBM Nairobi processor boasts a configuration of seven qubits, a standout attribute is its




Machine	#Qs	QV	Processors	CT Mode	\mathcal{E}_{RB1}	\mathcal{E}_{RB2}	\mathcal{E}_{SRB}	Topology
IBM Lima	5	8	Falcon r4T	Minor	0.004	0.026	1.2	
				Medium	0.007	0.023	3.4	
				Severe	0.010	0.037	5.6	
IBM Nairobi	7	32	Falcon r5.11H	Minor	0.006	0.006	1.6	
				Medium	0.007	0.009	2.15	
				Severe	0.009	0.012	2.7	
IBM Guadalupe	16	32	Falcon r4P	Minor	0.014	0.007	1.4	
				Medium	0.010	0.004	2.25	
				Severe	0.007	0.002	3.1	

Table 2: Characteristics of IBM quantum devices used in our study, IBM Lima, IBM Nairobi, and IBM Guadalupe. Each device has a different machine, number of qubits (#Qs), quantum volume (QV), processor, crosstalk mode (CT Mode), Error Per Gate of RB and SRB (\mathcal{E}_{RB1} , \mathcal{E}_{RB2} , and \mathcal{E}_{SRB}), and topology.

remarkable reduction in crosstalk errors. Adding to its technical capability, this processor is ingeniously arranged as an H processor type with higher levels of connectivity. The driving force behind this notable achievement lies in the quantum volume, which reaches an impressive 32. This substantial increase in quantum volume translates into a significant enhancement of error rates, particularly for crosstalk errors. The IBM Guadalupe system, featuring 16 qubits, was unveiled with the utilization of the latest heavy-hex lattice architecture. This configuration offers an enhanced quantum volume of 32. Structured in a Falcon r4P arrangement, the processors adopt a P processor type with reduced connectivity while increasing the number of qubits compared to the IBM Nairobi system. This consequence between topology connectivity and QV provides a compromise solution to the crosstalk error rates.

After we analyze the comparison between the IBM Lima 5, IBM Nairobi 7, and IBM Guadalupe 16 devices, it is evident that the selection of a specific device holds significant importance in the execution of various operations, notably in terms of quantum error mitigation (QEM) and quantum error correction (QEC). This comparison emphasizes the critical role that the choice of a quantum device plays in ensuring the efficacy and success of operations that involve error mitigation and correction within the quantum computing paradigm.

5.5 Impact of Crosstalk Error on Circuit Fidelity

Finally, we evaluate the crosstalk error for the most severe IBM Nairobi to determine its effect on the circuit fidelity. We choose four benchmarks from [51] like grover_n2, toffoli_n3, cat_state_n4, and Ipn_n5 with the different numbers of qubits and gates per benchmark. We prepare all experimental benchmarks at optimization level 0, which is no optimization for the simulation to determine the real effect of crosstalk error. The baseline is asynchronous CNOTs (no crosstalk) with the experimental benchmarks.

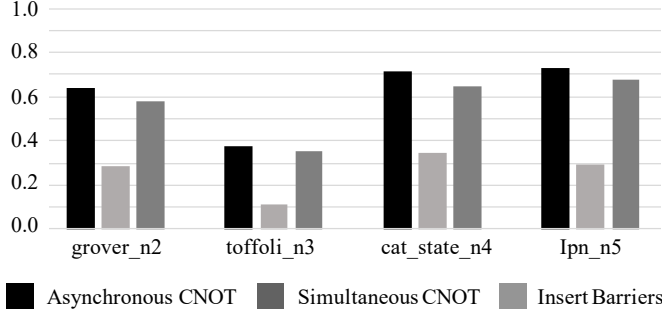


Fig. 7: Probability of Success Trails (PST) for 4 benchmarks under conditions with asynchronous CNOT, simultaneous CNOT, and insertion of the instruction barriers.

Figure 7 shows the impact of the crosstalk error of the Probability of Success Trails (PST) on the small-scale benchmarks of 2-5 qubits on the IBM Nairobi 7-qubits device. PST is the real system success probability of the number of trails with the correct measurement result divided by the total number of trails when executing on the real simulation. The probability of obtaining the right output state decreases with an increase in simultaneous CNOTs due to the inserted crosstalk error. Inserting the crosstalk error decreases the PST by 1.85x on average (up to 3.06x) based on the noise model of the tested pair. This experimental result is based on the highest crosstalk error pair in the crosstalk error model for IBM Nairobi.

In the case of grover_n1, the fidelity decreases by 44.05% compared with the non-crosstalk case. When we compare the presence of a barrier with no barrier in terms of output fidelity, the fidelity is improved by 2.06x. In the best case of toffoli_n3, the fidelity decreases by 30.54% and improves by 3.06x when a barrier is inserted. In the worst case, such as for cat_state_n4, the fidelity decreases by 48.35% compared with the non-crosstalk case. In our comparison in terms of output fidelity and circuit depth with and without a barrier, the fidelity improves by 1.87x. With Ipn_n5, the fidelity decreases by 40.21% with an improvement of 2.3x after the barrier is inserted.

As a consequence, the insertion of a barrier results in an improvement in the output fidelity up to almost the same level as that of no crosstalk errors. Therefore, this work may lead to a greater interest in QEM techniques in the future.

6 Discussion and Limitations

A recent trend in QEM techniques [52] is to exploit greater potential from the crosstalk error with a greater number of mitigation opportunities. Unlike innovations that are mostly driven by the underlying technologies, our study takes the first profound direction which is to enable a deeper understanding of the crosstalk error model for different devices by leveraging the RB and SRB protocols. Relatively little attention has been paid to this approach for two main reasons: 1) it is exceedingly difficult to extract useful information from a large number of circuit and gate sequences, which is the accurate level at which most operations today operate, and 2) the scalability of the

protocol on all different devices, which is an effective static analysis of a protocol, becomes quite difficult as the size of the operation matrix grows exponentially with the number of qubits. We believe that these are two critical yet difficult problems in the understanding of crosstalk error characteristics because they prevent the quantum operation from performing correctly.

Limited Value on a Realistic System: As the data are limited on realistic systems, specific details about the current state of IBM’s quantum devices and their performance with real-world data may not be available to all researchers. The progress made by and specifications for quantum devices is continuously evolving as research and development in quantum computing advance. To obtain the most accurate and up-to-date information about IBM’s quantum devices, including any limited crosstalk error from real systems, we used a fake device that mimics a real system. Additionally, due to the expensive runtime cost and the limits of crosstalk metric within the RB and SRB protocols on a real system, a fake device is preferable for this study.

Noise Beyond the NISQ Systems: Beyond the NISQ, the noise problem in quantum computing becomes more severe as researchers develop quantum components that are more fault-tolerant. QEC is paramount, and it demands additional qubits and computational resources. The challenges include mitigating decoherence and environmental interactions, reducing error rates, ensuring scalability while managing noise, improving quantum hardware, and refining noise models for accurate characterization. Strategies such as hybrid quantum-classical approaches may serve to address these challenges, as the field focuses on building robust, scalable quantum computers that are capable of handling errors effectively and enabling practical quantum information processing. However, our study experiments with the current NISQ devices, which have a different way of handling errors to explore more in the practical QIP.

Trade-off between Fidelity and Depth: Although the fidelity is enhanced because of the insertion barrier, the increase in circuit depth is not negligible. Fidelity is crucial to reliable quantum computation and represents the accuracy of quantum operations. However, the depth of the quantum circuit and the number of sequential quantum operations may be compromised to reduce the crosstalk error. This trade-off arises because mitigation techniques to counter crosstalk can lead to increased computational overhead and decreased depth. Researchers are exploring innovative techniques and error-mitigation strategies that maintain an equilibrium between fidelity and depth to ensure the efficient functioning of quantum circuits while effectively suppressing the disruptive effects of crosstalk.

Mitigation Opportunity: Mitigating crosstalk errors provides a valuable opportunity to enhance the robustness and reliability of QIP. By identifying and implementing effective mitigation strategies, researchers can significantly minimize the impact of crosstalk, thereby improving the overall performance of quantum circuits. Opportunities for mitigation crosstalk include the development of error correction codes, optimized control mechanisms, and advanced calibration techniques. Moreover, leveraging QEC methods can help counteract the undesirable effects of crosstalk by preserving the integrity of quantum states during computation. As quantum computing technologies advance, exploring novel mitigation opportunities will be crucial

to unlocking the full potential of quantum systems and ensuring their viability in practical applications in the future to bridge between NISQ and FTQC.

7 Conclusion and Outlook

Crosstalk errors present a significant challenge in Noisy Intermediate-Scale Quantum (NISQ) devices, compromising the execution fidelity of quantum operations. In this work, we propose a method to efficiently estimate the crosstalk error from the correlation controlled-NOT (CNOT) gate by combining Randomized Benchmarking (RB) and Simultaneous Randomized Benchmarking (SRB) on different quantum device properties. This involves preprocessing the device property to determine each CNOT correlation pair. To quantify the effect of crosstalk errors on the NISQ devices, we leverage Randomized Benchmarking (RB) and Simultaneous Randomized Benchmarking (SRB) protocol. It enables the accurate estimation of CNOT errors by measuring average gate performance by running sequences of random Clifford group gates. Sequentially, we can derive the crosstalk error rate on different devices. Experimental results demonstrate comprehensive error information for each device as a crosstalk error model, its daily variation, and a comparison between the three devices. Additionally, we evaluate the impact of crosstalk error on several small-scale benchmarks to determine the improvements in circuit fidelity brought about by the insertion of an instruction barrier. Our proposed method could be extended to different device properties by configuring the topology correlation of the crosstalk error pairs. Our work confirms that these protocols can address the crosstalk error model on different devices and a straightforward estimation protocol in a more effective, scalable, and better reconfigurable method. Future work on analytically bounding the number of iterations could demonstrate the performance of this method against well-known characterization techniques. We believe that the results explored in this study would promote future work in the direction of exploring the crosstalk error model and further investigations into quantum error mitigation techniques.

Acknowledgments. This research was partly supported by Quantum Computing based on Quantum Advantage challenge research (RS-2023-00257994) through the National Research Foundation of Korea (NRF) funded by the Korean government (MSIT) and Institute for Information & communications Technology Planning & Evaluation (IITP) grant funded by the Korea government (MSIT) (No. 2020-0-00014, A Technology Development of Quantum OS for Fault-tolerant Logical Qubit Computing Environment).

References

- [1] Choi, C.Q.: Ibm’s quantum leap: The company will take quantum tech past the 1,000-qubit mark in 2023. *IEEE Spectrum* **60**(1), 46–47 (2023)
- [2] Arute, F., Arya, K., Babbush, R., Bacon, D., Bardin, J.C., Barends, R., Biswas, R., Boixo, S., Brandao, F.G., Buell, D.A., *et al.*: Quantum supremacy using a programmable superconducting processor. *Nature* **574**(7779), 505–510 (2019)

- [3] Gustafson, E.J., Li, A.C., Khan, A., Kahn, A., Kim, J., Kurkcuoglu, D.M., Alam, M.S., Orth, P.P., Rahmani, A., Iadecola, T.: Preparing quantum many-body scar states on quantum computers. Technical report, Fermi National Accelerator Lab.(FNAL), Batavia, IL (United States) (2023)
- [4] Riel, H.: Quantum computing technology. In: 2021 IEEE International Electron Devices Meeting (IEDM), pp. 1–3 (2021). IEEE
- [5] Xu, C., Szefer, J.: Long-term analysis of the dependability of cloud-based nisq quantum computers. In: Proceedings of the 18th International Conference on Availability, Reliability and Security, pp. 1–6 (2023)
- [6] Alvarado-Valiente, J., Romero-Álvarez, J., Moguel, E., García-Alonso, J., Murillo, J.M.: Technological diversity of quantum computing providers: a comparative study and a proposal for api gateway integration. *Software Quality Journal*, 1–21 (2023)
- [7] Noiri, A., Takeda, K., Nakajima, T., Kobayashi, T., Sammak, A., Scappucci, G., Tarucha, S.: Fast universal quantum gate above the fault-tolerance threshold in silicon. *Nature* **601**(7893), 338–342 (2022)
- [8] Hashim, A., Seritan, S., Proctor, T., Rudinger, K., Goss, N., Naik, R.K., Kreikebaum, J.M., Santiago, D.I., Siddiqi, I.: Benchmarking quantum logic operations relative to thresholds for fault tolerance. *npj Quantum Information* **9**(1), 109 (2023)
- [9] Postler, L., Heußen, S., Pogorelov, I., Rispler, M., Feldker, T., Meth, M., Marciniak, C.D., Stricker, R., Ringbauer, M., Blatt, R., *et al.*: Demonstration of fault-tolerant universal quantum gate operations. *Nature* **605**(7911), 675–680 (2022)
- [10] Zhao, P., Linghu, K., Li, Z., Xu, P., Wang, R., Xue, G., Jin, Y., Yu, H.: Quantum crosstalk analysis for simultaneous gate operations on superconducting qubits. *PRX quantum* **3**(2), 020301 (2022)
- [11] Ash-Saki, A., Alam, M., Ghosh, S.: Analysis of crosstalk in nisq devices and security implications in multi-programming regime. In: Proceedings of the ACM/IEEE International Symposium on Low Power Electronics and Design, pp. 25–30 (2020)
- [12] Murali, P., McKay, D.C., Martonosi, M., Javadi-Abhari, A.: Software mitigation of crosstalk on noisy intermediate-scale quantum computers. In: Proceedings of the Twenty-Fifth International Conference on Architectural Support for Programming Languages and Operating Systems, pp. 1001–1016 (2020)
- [13] Gaebler, J.P., Baldwin, C.H., Moses, S.A., Dreiling, J.M., Figgatt, C., Foss-Feig, M., Hayes, D., Pino, J.M.: Suppression of midcircuit measurement crosstalk errors

- with micromotion. *Phys. Rev. A* **104**, 062440 (2021) <https://doi.org/10.1103/PhysRevA.104.062440>
- [14] McKay, D.C., Cross, A.W., Wood, C.J., Gambetta, J.M.: Correlated randomized benchmarking. arXiv preprint arXiv:2003.02354 (2020)
 - [15] Sarovar, M., Proctor, T., Rudinger, K., Young, K., Nielsen, E., Blume-Kohout, R.: Detecting crosstalk errors in quantum information processors. *Quantum* **4**, 321 (2020)
 - [16] Niu, S., Todri-Sanial, A.: Analyzing crosstalk error in the nisq era. In: 2021 IEEE Computer Society Annual Symposium on VLSI (ISVLSI), pp. 428–430 (2021). IEEE
 - [17] Rudinger, K., Hogle, C.W., Naik, R.K., Hashim, A., Lobser, D., Santiago, D.I., Grace, M.D., Nielsen, E., Proctor, T., Seritan, S., *et al.*: Experimental characterization of crosstalk errors with simultaneous gate set tomography. *PRX Quantum* **2**(4), 040338 (2021)
 - [18] Seo, S., Bae, J.: Measurement crosstalk errors in cloud-based quantum computing. *IEEE Internet Computing* **26**(1), 26–33 (2021)
 - [19] Ding, Y., Gokhale, P., Lin, S.F., Rines, R., Propson, T., Chong, F.T.: Systematic crosstalk mitigation for superconducting qubits via frequency-aware compilation. In: 2020 53rd Annual IEEE/ACM International Symposium on Microarchitecture (MICRO), pp. 201–214 (2020). IEEE
 - [20] Ash-Saki, A., Alam, M., Ghosh, S.: Experimental characterization, modeling, and analysis of crosstalk in a quantum computer. *IEEE Transactions on Quantum Engineering* **1**, 1–6 (2020)
 - [21] Razif, R.A.M., Maharum, S.M.M., Hasani, A.H., Mansor, Z.: Mitigation techniques for crosstalk in ics. In: IOP Conference Series: Materials Science and Engineering, vol. 701, p. 012037 (2019). IOP Publishing
 - [22] Winick, A., Wallman, J.J., Emerson, J.: Simulating and mitigating crosstalk. *Physical review letters* **126**(23), 230502 (2021)
 - [23] Xie, L., Zhai, J., Zheng, W.: Mitigating crosstalk in quantum computers through commutativity-based instruction reordering. In: 2021 58th ACM/IEEE Design Automation Conference (DAC), pp. 445–450 (2021). IEEE
 - [24] Gambetta, J.M., Córcoles, A.D., Merkel, S.T., Johnson, B.R., Smolin, J.A., Chow, J.M., Ryan, C.A., Rigetti, C., Poletto, S., Ohki, T.A., Ketchen, M.B., Steffen, M.: Characterization of addressability by simultaneous randomized benchmarking. *Phys. Rev. Lett.* **109**, 240504 (2012) <https://doi.org/10.1103/PhysRevLett.109.240504>

- [25] Marella, S.T., Parisa, H.S.K.: Introduction to quantum computing. *Quantum Computing and Communications* (2020)
- [26] Chae, E., Choi, J., Kim, J.: An elementary review on basic principles and developments of qubits for quantum computing. *Nano Convergence* **11**(1), 1–13 (2024)
- [27] Shukla, A., Vedula, P.: An efficient quantum algorithm for preparation of uniform quantum superposition states. *Quantum Information Processing* **23**(2), 38 (2024)
- [28] Renner, M.J., Brukner, Č.: Computational advantage from a quantum superposition of qubit gate orders. *Physical Review Letters* **128**(23), 230503 (2022)
- [29] Ivanov, P.A., Vitanov, N.V.: Two-qubit quantum gate and entanglement protected by circulant symmetry. *Scientific Reports* **10**(1), 5030 (2020)
- [30] Krasnok, A., Dhakal, P., Fedorov, A., Frigola, P., Kelly, M., Kutsaev, S.: Superconducting microwave cavities and qubits for quantum information systems. *Appl Phys Rev* **11** (2024)
- [31] Zheng, M., Li, A., Terlaky, T., Yang, X.: A bayesian approach for characterizing and mitigating gate and measurement errors. *ACM Transactions on Quantum Computing* **4**(2), 1–21 (2023)
- [32] Selvarajan, R., Dixit, V., Cui, X., Humble, T.S., Kais, S.: Prime factorization using quantum variational imaginary time evolution. *Scientific reports* **11**(1), 20835 (2021)
- [33] Russo, V., Mari, A., Shammah, N., LaRose, R., Zeng, W.J.: Testing platform-independent quantum error mitigation on noisy quantum computers. *IEEE Transactions on Quantum Engineering* (2023)
- [34] Niu, S., Todri-Sanial, A.: Enabling multi-programming mechanism for quantum computing in the nisq era. *Quantum* **7**, 925 (2023)
- [35] Hua, F., Wang, M., Li, G., Peng, B., Liu, C., Zheng, M., Stein, S., Ding, Y., Zhang, E.Z., Humble, T.S., et al.: Qasmtrans: A qasm based quantum transpiler framework for nisq devices. *arXiv preprint arXiv:2308.07581* (2023)
- [36] Mathur, N., Landman, J., Li, Y.Y., Strahm, M., Kazdaghli, S., Prakash, A., Kerenidis, I.: Medical image classification via quantum neural networks. *arXiv preprint arXiv:2109.01831* (2021)
- [37] Mensa, S., Sahin, E., Tacchino, F., Kl Barkoutsos, P., Tavernelli, I.: Quantum machine learning framework for virtual screening in drug discovery: a prospective quantum advantage. *Machine Learning: Science and Technology* **4**(1), 015023 (2023)

- [38] Baheri, B., Chen, D., Fang, B., Stein, S.A., Chaudhary, V., Mao, Y., Xu, S., Li, A., Guan, Q.: Tqea: Temporal quantum error analysis. In: 2021 51st Annual IEEE/IFIP International Conference on Dependable Systems and Networks-Supplemental Volume (DSN-S), pp. 65–67 (2021). IEEE
- [39] Yetis, H., Karakoes, M.: Investigation of noise effects for different quantum computing architectures in ibm-q at nisq level. In: 2021 25th International Conference on Information Technology (IT), pp. 1–4 (2021). IEEE
- [40] Martina, S., Buffoni, L., Gherardini, S., Caruso, F.: Learning the noise fingerprint of quantum devices. *Quantum Machine Intelligence* **4**(1), 8 (2022)
- [41] Helsen, J., Roth, I., Onorati, E., Werner, A.H., Eisert, J.: General framework for randomized benchmarking. *PRX Quantum* **3**(2), 020357 (2022)
- [42] Hines, J., Lu, M., Naik, R.K., Hashim, A., Ville, J.-L., Mitchell, B., Kriekebaum, J.M., Santiago, D.I., Seritan, S., Nielsen, E., *et al.*: Demonstrating scalable randomized benchmarking of universal gate sets. *Physical Review X* **13**(4), 041030 (2023)
- [43] Mills, A.R., Guinn, C.R., Gullans, M.J., Sigillito, A.J., Feldman, M.M., Nielsen, E., Petta, J.R.: Two-qubit silicon quantum processor with operation fidelity exceeding 99%. *Science Advances* **8**(14), 5130 (2022)
- [44] Liu, R., Guan, Z., Cheng, X., Zhu, P., Feng, S.: Suppression of crosstalk in quantum computers based on instruction exchange rules and duration. In: *Journal of Physics: Conference Series*, vol. 2524, p. 012026 (2023). IOP Publishing
- [45] Guan, Z., Liu, R., Cheng, X., Feng, S., Zhu, P.: Suppression of crosstalk in quantum circuit based on instruction exchange rules and duration. *Entropy* **25**(6), 855 (2023)
- [46] White, G.A., Pollock, F.A., Hollenberg, L.C., Modi, K., Hill, C.D.: Non-markovian quantum process tomography. *PRX Quantum* **3**(2), 020344 (2022)
- [47] Pereira, L., García-Ripoll, J.J., Ramos, T.: Parallel tomography of quantum non-demolition measurements in multi-qubit devices. *npj Quantum Information* **9**(1), 22 (2023)
- [48] Khadirsharbiyani, S., Sadeghi, M., Zarch, M.E., Kotra, J., Kandemir, M.T.: Trim: crosstalk-aware qubit mapping for multiprogrammed quantum systems. In: 2023 IEEE International Conference on Quantum Software (QSW), pp. 138–148 (2023). IEEE
- [49] Wei, K.X., Magesan, E., Lauer, I., Srinivasan, S., Bogorin, D.F., Carnevale, S., Keefe, G.A., Kim, Y., Klaus, D., Landers, W., Sundaresan, N., Wang, C., Zhang, E.J., Steffen, M., Dial, O.E., McKay, D.C., Kandala, A.: Hamiltonian engineering

with multicolor drives for fast entangling gates and quantum crosstalk cancellation. *Phys. Rev. Lett.* **129**, 060501 (2022) <https://doi.org/10.1103/PhysRevLett.129.060501>

- [50] Finck, A., Carnevale, S., Klaus, D., Scerbo, C., Blair, J., McConkey, T., Kurter, C., Carniol, A., Keefe, G., Kumph, M., *et al.*: Suppressed crosstalk between two-junction superconducting qubits with mode-selective exchange coupling. *Physical Review Applied* **16**(5), 054041 (2021)
- [51] Li, A., Stein, S., Krishnamoorthy, S., Ang, J.: Qasmbench: A low-level quantum benchmark suite for nisq evaluation and simulation. *ACM Transactions on Quantum Computing* **4**(2) (2023) <https://doi.org/10.1145/3550488>
- [52] Sun, J., Yuan, X., Tsunoda, T., Vedral, V., Benjamin, S.C., Endo, S.: Mitigating realistic noise in practical noisy intermediate-scale quantum devices. *Physical Review Applied* **15**(3), 034026 (2021)